Journal of Thermal Analysis and Calorimetry, Vol. 96 (2009) 2, 645–651

FIRST PRINCIPLES STUDIES OF THERMAL DECOMPOSITION OF ANHYDROUS ZINC OXALATE

A. Koleżyński and A. Małecki*

AGH University of Science and Technology, Faculty of Materials Science and Ceramics, Al. Mickiewicza 30
30-059 Cracow, Poland

The results of first principles calculations of band structure, density of states and electron density topology of ZnC_2O_4 crystal are presented. The calculations have been performed with WIEN2k FP LAPW *ab initio* package. The obtained SCF electron density has been used in calculations of Bader's QTAIM (quantum theory of atoms in molecules) topological properties of the electron density in crystal. Additional calculations of bond orders (Pauling, Bader, Cioslowski and Mixon) and bond valences according to bond valence model have been done. The obtained results are analyzed from the point of view of the thermal decomposition process, and this analysis indicates, that most probably this compound should decompose to metal oxide, carbon oxide and carbon dioxide, in agreement with the experiment.

Keywords: *bond order, bond valence, electron density topology, FP-LAPW ab initio calculations, thermal decomposition*

Introduction

Anhydrous zinc oxalate belongs to the isostructural family of anhydrous metal oxalates β-MC_2O_4 (where *M* is Fe, Co, Ni, Zn, Cu – Kondrashev *et al.* [1]; Cd – Jeanneau *et al.* [2]), with monoclinic unit cell $P2_1/n$, with similar cell parameters, arrangement of the MO_6 octahedra and oxalate anions, but different thermal decomposition to M, MO or MCO_3 [3–11]. Since there is still lack of consistent description and explanation of the origin and thermal decomposition path in given oxalate, the theoretical analysis of the electronic properties based on the *ab initio* calculations can give additional insight into the thermal decomposition process and help not only to explain thermal decomposition path in given oxalate, but also to predict such most probably path for the compound for which experimental results are unavailable.

In this paper we present the results of the theoretical studies undertaken for anhydrous zinc oxalate. The obtained results of the *ab initio* electronic structure calculations, bond orders and bond valences are discussed in the light of the thermal decomposition process.

Computational details

The *ab initio* calculations of the electron density topology, band structure and density of states in ZnC_2O_4 crystal, have been performed using WIEN2k FP-LAPW *ab initio* package [12] within density functional theory (DFT) formalism [13–18]. As in our previous calculations performed for cadmium and silver oxalates [19], 500 *k*-points (7×7×8 mesh within the irreducible Brillouin zone), cut-off parameter Rk_{max}=7.5 and GGA-PBE exchange-correlation potential [20], have been chosen for calculations. The values of muffin-tin radii (R_i) were set to [a.u.]: Zn – 1.7, O – 1.08, C – 1.08. The following convergence criteria for SCF calculations: $\Delta E_{SCF} \leq 10^{-5}$ Ry for total energy and $\Delta\rho_{SCF} \leq 10^{-5}$ e for electron density topology analysis has been chosen. The band structure was calculated for selected high symmetry points defined for monoclinic unit cell (Group no. 14 on Bilbao Crystallographic Server http://www.cryst.ehu.es).

Based on the SCF electron density distribution in crystal cell, the topological properties of bond critical points has been calculated (within Bader's quantum theory of atoms in molecules [21] formalism). According to his formulation, every bond critical point BCP, can be described by its position, electron density in this point, Hessian matrix eigenvalues λ_1, λ_2, λ_3 and Laplacian $\nabla^2\rho(r)$, defined as a trace of Hessian matrix and these parameters allow to characterize bond properties, among the others the bond character (covalent, ionic, etc.) and bond ellipticity (thus its π-character). The results of the *ab initio* calculations have been used in calculations of bond orders as defined by Pauling [22], Bader [23], Cioslowski and Mixon [24] and Jules and Lombardi [25] and bond va-

* Author for correspondence:

1388–6150/$20.00

Akadémiai Kiadó, Budapest, Hungary
Springer, Dordrecht, The Netherlands

lences, according to the bond valence method (an excellent review of BVM can be found in Brown [26]). The more detailed description of methods used in present calculations can be found in our previous papers [19, 27].

Zinc oxalate structure

Zinc oxalate can be described [1] as built from chains (Fig. 1) $–C_2O_4–Zn–C_2O_4–Zn–$, or alternatively as layered material, formed by cationic layers built from corner-shared ZnO_6 octahedra, linked together via bidentate chelating oxalate groups. Each zinc atom is surrounded by six oxygen atoms, all belonging to oxalate groups: two O_1 and four O_2 atoms, forming highly distorted octahedron (Fig. 2) with 3 different Zn–O distances (1.946, 2.055 and 2.317 Å). All octahedra are connected by corners; in each zinc octahedron, all four O_2 atoms are shared by two octahedra, belonging to neighboring chains, almost perpendicular to each other (Fig. 2). The oxalate group is distorted – the angle between carboxide group and C–C bond is about 22°. The crystal structure parameters and fractional atomic coordinates, used in *ab initio* calculations are listed in Table 1.

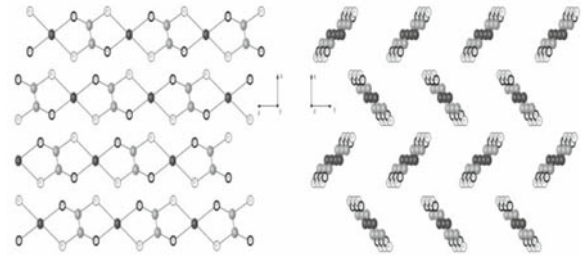

Fig. 1 Anhydrous zinc oxalate chain structure projected onto *xz* and *xy* planes. In the right figure, the plane is slightly rotated in *x* direction to show the chains spatial orientation (chains are parallel to *z*-axis). Atoms are represented by circles identical as at Fig. 2

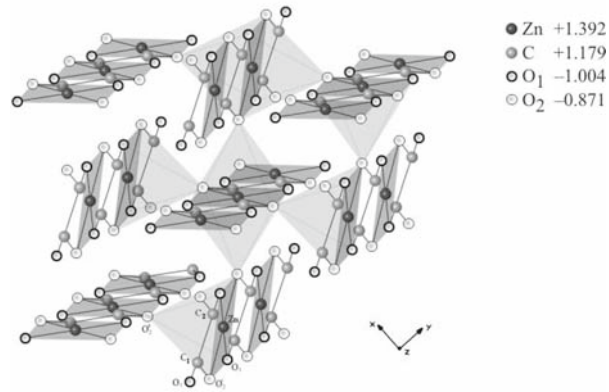

Fig. 2 Anhydrous zinc oxalate crystal structure. Calculated Bader's QTAiM total charges for the atoms are presented in upper right corner of the figure

Results and discussion

The band structure of zinc oxalate (Fig. 3) contains 50 valence bands; calculated Fermi energy and direct band gap are 0.26793 and 0.173 Ry respectively (in case of cadmium oxalate [19] we had 52 valence bands, E_F=0.26882 Ry, indirect band gap 0.246 Ry, so the Fermi energies are almost identical, while band gaps differ by one third). Despite the known fact, that Fermi energies and band gaps calculated with this method are often in disagreement with experimental values, they can be used for comparison with respective values calculated for similar compounds. Thus based on their calculated band structures, taking into account that zinc and cadmium have similar electronic configuration – both are closed shell $d^{10}s^2$ elements – but different size (zinc atomic radius is much smaller) and their anhydrous oxalates are isostructural crystals, it is likely, that they will have significantly different properties in these crystals (as this exceeds the scope of this paper, more detailed analysis of band structure including band characters and occupancies will be published elsewhere). This supposition has strong support in calculated density of states. Figures 4 and 5 show the total and partial densities of states for the individual atoms in zinc ox-

Table 1 Anhydrous zinc oxalate experimental crystal structure data and fractional atomic coordinates [1]

Structure	Space group	*a*/Å	*b*/Å	*c*/Å	β/°	*V*/Å^3
ZnC_2O_4	$P2_1/n$	5.831	5.123	5.331	113.20	146.37

Fractional atomic coordinates

Atom symbol	*X*	*Y*	*Z*
Zn	0	0	0
O_1	0.17990	0.19590	0.36110
O_2	0.13980	0.18690	0.77510
C	0.07314	0.12817	0.54821

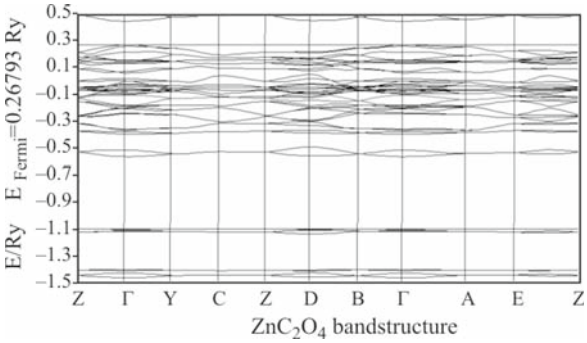

Fig. 3 Band structure calculated for zinc oxalate

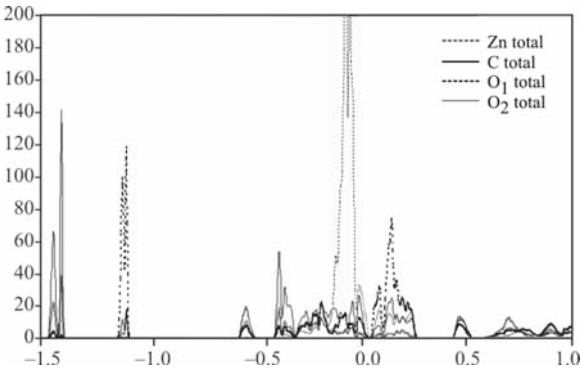

Fig. 4 Total density of states calculated for anhydrous zinc oxalate (only total DOS-es for individual atoms are shown in the picture)

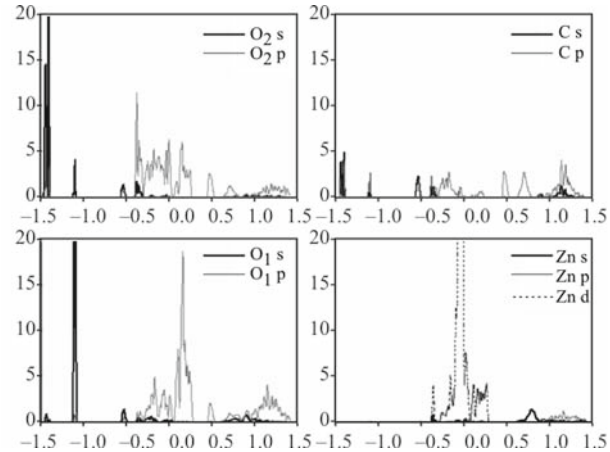

Fig. 5 Partial density of states, calculated for anhydrous zinc oxalate

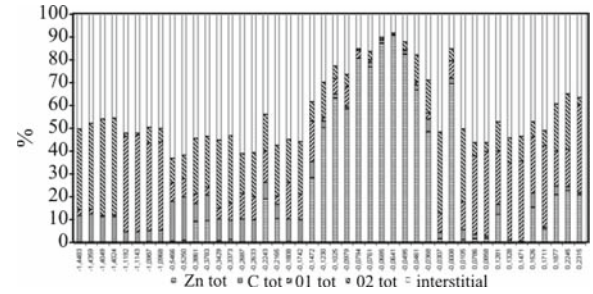

Fig. 6 Bands characters calculated for zinc oxalate, for highest symmetry point Γ

alate crystal. For the total DOS, one can find three sharp peaks in valence region. The carbon 2s and 2p electrons are mixed with O_1 and O_2 oxygen 2s electrons in two peaks (carbon 2s electrons mainly at about –1.45 Ry and carbon 2p electrons at about –1.45 and –1.1 Ry). The 2s electrons of O_1 are mixed with carbon electrons almost entirely in peak located at about –1.1 Ry, while the same electrons originating from O_2 are mixed in peak at about –1.45 Ry. The next small peak at about –0.55 Ry consists of comparable amounts of 2s and 2p electrons from carbon and both oxygen atoms.

There are also two broader regions with filled states up to Fermi level. The first one broader, built up from zinc 3d electrons, mixed with carbon 2p, O_2 oxygen 2p and to some extent with O_1 oxygen 2p electrons; the narrower one consists of zinc 3d, carbon 2p and O_1 2p electrons with small participation of O_2 2p electrons. In conduction region there are mainly mixed states of oxygen 2p, carbon 2p and metal s electrons. The total and partial DOS pictures shows high asymmetry in localization of 2s and 2p states, related to inequivalent O_1 and O_2 atoms, thus one can expect significant differences in properties of bonds formed by these oxygen atoms.

The spatial characters of individual bands change not only from band to band, but also for different directions in reciprocal lattice, so we will not go into details here, but some insight can be obtained from the analysis of bands characters for the most symmetric *k* point –Γ point. On Fig. 6, such characters are presented in the form of cumulative histogram, where each band is represented by one bar filled with percentage number of electrons originating from individual atoms adding up to 100% (with delocalized electrons off the bands). Such approach is complementary to the DOS picture, and it is clearly visible, that there are few bands dominated by zinc 3d electrons, with small participation of oxygen electrons, and the dominating rest of the bands, where the electrons from oxygen are mixed with those from carbon. One can see also the strong asymmetry in bands occupation by the electrons from two types of oxygen atoms in zinc oxalate structure, in contrast to bands character in cadmium oxalate.

The band structure and density of states calculated for zinc oxalate suggest, that zinc atom is almost entirely interacting with oxygen atoms, and the two symmetrically inequivalent O_1 and O_2 oxygen atoms,

are experiencing different influence of the surroundings, and therefore different bonding properties.

The electron density distribution obtained from the SCF calculations was used in Bader's QTAiM analysis of electron density topology. The respective results are presented in Table 2, and the values of calculated total charges are presented on Fig. 2. These results show that the value of electron density in bond critical points BCP is largest for C_1–O_1 bond, then smaller but comparable in value for C_1–O_2^i and C_1–C_2 bonds and much smaller for zinc oxygen bonds, but again greater for Zn–O_1 and smaller for both Zn–O_2 bonds. Thus the C_1–O_1 bond is the strongest one, the strength of C_1–O_2^i and C_1–C_1 bonds is similar and the weakest bonds are created by zinc and oxygen atoms. Additionally the calculated ellipticity indicates some π-character of C_1–O_1, C_1–O_2^i and C_1–C_2 bonds. This allows us to suppose, that during thermal decomposition process, as the first one, the one of the two longest Zn–O_2^{ii} bonds will be broken.

Since O_2^{ii} atom is corner-shared by two octahedra (Fig. 2), this will be followed by the process of shortening (and thus strengthening) of Zn–O_2^{ii} and C–O_2^{ii} bonds in neighboring octahedron in which O_2^{ii} atom remains and in the same time, the electron flow and substantial change in electron charge distribution. Since the difference in electron densities and Laplacian values in bond critical points calculated for both Zn–O_2^i and Zn–O_1 bonds (Table 2) are similar, therefore the process of structure reconfiguration after breaking the first Zn–O_2^{ii} bond will probably result in greater strength of Zn–O_2^i bond, than Zn–O_1 bond. Hence, since the C_1–O_2^i bond is slightly stronger than C_1–C_2 bond, we may assume the following sequence of consecutive bond breaking: Zn–O_2^{ii}, Zn–O_1 (O_1 from neighboring octahedron, bonded to C_1 from analyzed octahedron) and C_1–C_2, and as the result – free CO_2 molecule is created. This leads to shortening of the rest of bonds in the octahedron and from this point, the analysis based on the electron density properties at BCP, can not be conclusive due to the lack of the respective data about the changes of electron topology after breaking the weakest bond. To make the analysis more complete, we have performed the calculations of bond order and bond valences, to get additional information about the bonds properties in analyzed structure.

In Table 3, the calculated bond orders, as defined by Pauling [22], Bader [23], Cioslowski and Mixon [24] (with parameters obtained by Howard and Lamarche [28]) and Jules and Lombardi [25], are shown (more detailed description of these bond orders has been presented elsewhere [27]). The obtained results confirm the picture emerging from topological analysis and show, that in all cases, the C_1–O_1 bond is strongest, then much weaker are C_1–O_2^i and C_1–C_2 bonds (the latter one is little stronger) and the weakest (except for n_{CM} case) are Zn–O bonds. Again this allows us to suppose that in process of thermal decomposition, the above mentioned bond breaking sequence, leading to freeing of CO_2 molecule, will take place. The bond order analysis provides us some extra clarification, concerning the next steps of decomposition process. Since, as it results from most reliable bond orders calculated from electron density topology (Howard and Lamarche definition, based on Cioslowski and Mixon proposition – detailed analysis in [27]), bond orders of C_1–O_2^i, Zn–O_1 and Zn–O_2^i are comparable (in case of $n_{CM(HL)}$ the Zn–O bonds orders are even greater than the one for C_1–O_2^i), thus we can suppose, that as next ones, the C_1–O_2^i, than Zn–O_1 bonds will be broken, leaving Zn–O_2^i and C_1–O_1 bonds unbroken. Eventu-

Table 3 Bond orders calculated from theoretical electron density bond critical points parameters for anhydrous zinc oxalate

	ZnC_2O_4	n_P	n_B	$n_{CM(HL)}$	$n_{B(JL)}$
r_1	Zn–O_1	0.24	0.52	0.95	0.65
r_2	Zn–O_2^i	0.18	0.49	0.91	0.60
r_3	Zn–O_2^{ii}	0.10	0.44	0.84	0.51
r_4	C_1–O_1	1.62	1.72	1.60	2.56
r_5	C_1–O_2^i	0.87	0.94	0.89	1.07
r_6	C_1–C_2	0.94	1.08	0.91	1.16

Table 2 Topological properties of bond critical points calculated for electron density obtained in FP_LAPW ab initio calculations for anhydrous zinc oxalate

	ZnC_2O_4	R_{AB}/ Å	R_A/ Å	R_B/ Å	λ_1/ Å^{-5}	λ_2/ Å^{-5}	λ_3/ Å^{-5}	ρ_{BCP}/ e Å^{-3}	$\nabla^2\rho(r)$/ Å^{-5}	ε
r_1	Zn–O_1	1.9465	0.9532	0.9933	–3.2558	–3.2414	16.0598	0.6163	9.5630	0.0045
r_2	Zn–O_2^i	2.0548	0.9953	1.0595	–2.4172	–2.3767	11.7123	0.4990	6.9160	0.0170
r_3	Zn–O_2^{ii}	2.3174	1.1241	1.1933	–1.1021	–1.0806	5.4561	0.2714	3.2730	0.0198
r_4	C_1–O_1	1.1551	0.3891	0.7660	–35.5465	–33.3052	74.0330	3.2041	5.1960	0.0673
r_5	C_1–O_2^i	1.4114	0.5582	0.8532	–14.5945	–12.5895	9.9916	1.9010	–17.1920	0.1593
r_6	C_1–C_2	1.5398	0.7699	0.7699	–13.0136	–11.9340	10.2856	1.7168	–14.6620	0.0905

ally this process will lead to the decomposition of the anhydrous zinc oxalate to $ZnO+CO+CO_2$, in agreement with the experiment.

Another very useful inorganic chemistry concept we have used to support this analysis is bond valence. This concept, introduced by Pauling [22] binds the strength of chemical bond with its length, and the 'experimental' values of bond valences s_{ij} can be easily calculated from experimental bond lengths. The sum of the experimental bond valences $\sum s_{ij}^{exp}$ will not, in general, fulfill the valence sum rule, i.e. will not be exactly equal to the atomic valence V_i. The difference between the 'experimental' atomic valence $\sum s_{ij}^{exp}$ and the expected value V_i,

$$d_i = V_i - \sum_j s_{ij}'$$

can be used for calculating the reliability factor of the crystal structure. The root-mean-square average of the d_i values gives us a convenient measure of the agreement over the whole structure:

$$D = \sqrt{\langle d_i^2 \rangle}$$

The values of d_i and D greater than 0.1 v.u. indicate the existence of strained bonds, which can lead to instabilities in the crystal and show most strained regions in the structure. In Table 4, the calculated bond valences and residual strain factors and in Table 5 the theoretical bond valences and lengths are presented (again – more detailed description of the calculations based on this concept has been presented in our previous paper [27]).

The obtained results show, that the overall structure is highly strained (D=0.34 v.u.), and the highest strains d_i in the structure are associated with both oxygen atoms (–0.46 and 0.48 v.u.). The respective values for zinc and carbon environments are much smaller. As follow from Table 5, the discrepancy between theoretical (calculated from theoretical valences obtained via the electroneutrality sum rule) and experimental bond lengths is highest for $Zn–O_2^{ii}$ and $C–O_2^{i}$ bonds (~ 9%) – both bonds are to long, and for $Zn–O_1$ bond (~7.8%), which is to short, thus $Zn–O_1$ and $Zn–O_2^{ii}$ are under the influence of opposite strains. The differences are much smaller for the rest of the bonds, and in case of carbon–carbon bond there is practically no deviation from the theoretical value, predicted for this particular structure. These results suggest, that most reactive will be O_2 site – breaking the $Zn–O_2^{ii}$ bond (the weakest one) will result in highest decrease in overall strain field in the structure, shortening the $C_1–O_2^{ii}$ and lengthening $C_1–O_1$ bonds. Since $C_1–C_2$ bond has almost perfect length, it will

Table 4 Bond valences with residual strain factors d_i and D, calculated from BVM for zinc oxalate

		Bond length/Å / bond valence			V_{ij}	d_i	D
		$2O_1$	$2O_2^i$	$2O_2^{ii}$			
Zn	R_{exp}	1.9465	2.0548	2.3174			
	s_{ij}	0.5193	0.3874	0.1906	2.1945	–0.1945	0.3464
		C	Zn				
O_1	R_{exp}	1.1551	1.9465				
	s_{ij}	1.8869	0.5193		2.4635	–0.4635	
		C	Zn	Zn			
O_2	R_{exp}	1.4114	2.0548	2.3174			
	s_{ij}	0.9437	0.3874	0.1906	1.5217	0.4783	
		O_1	O_2	C			
C	R_{exp}	1.1551	1.4114	1.5398			
	s_{ij}	1.8869	0.9437	1.0006	3.8291	0.1709	

Table 5 Theoretical bond valences and bond lengths calculated from BVM for zinc oxalate

		s_{ij}^{theor}	R_{theor}/Å	R_{exp}/Å	$\Delta R/R$/%	Valence sum rule
r_1	$Zn–O_1$	⅓	2.1105	1.9465	7.77	
r_2	$Zn–O_2^i$	⅓	2.1105	2.0548	2.64	$Zn=2r_1+2r_2+2r_3=2\cdot⅓+2\cdot⅓+2\cdot⅓=2$
r_3	$Zn–O_2^{ii}$	⅓	2.1105	2.3174	8.93	$O_1=r_1+r_4=⅓+1⅔=2$
r_4	$C_1–O_1$	1⅔	1.2010	1.1551	3.82	$O_2=r_2+r_3+r_5=⅓+⅓+1⅓=2$
r_5	$C_1–O_2^i$	1⅓	1.2836	1.4114	9.05	$C=r_4+r_5+r_6=1⅔+1⅓+1=4$
r_6	$C_1–C_2$	1	1.5400	1.5398	0.01	

stay here unchanged and its breaking will not influence much the surroundings. This finding supports strongly the prediction we made earlier, that at this stage of decomposition process it is likely, that the CO_2 molecule will be freed. Similar analysis applies to the next steps in bond breaking process.

As another indicator of bond strain, the difference between the theoretically predicted and experimentally observed bond lengths can be used. In this case, the strain factor δ for a certain group of bonds or the structure as a whole can be described by following formula:

$$\delta = \sqrt{\frac{\sum_{n=1}^{N}\left(s_{ij}^{theor} - s_{ij}^{exp}\right)^2}{N}}$$

While d_i indicates the magnitude of unbalanced charge for given atom in the structure, the strain factor δ provides additional information about the differences in strains acting on single bonds or group of bonds. In Table 6, the values of bonds strain factors δ calculated for zinc oxalate are shown. Presented results indicate, that overall strains in the structure are significant, and the highest strains act on C–O_2 bonds. The strains acting on Zn–O bonds are much smaller and comparable to C–O_1 bond strains. Thus it follows, that energetically most favorable should be breaking or resizing of the C–O_2 bond. The presented results show, that BVM, based on the compound's geometry, confirms the conclusion we have drawn from *ab initio* calculated theoretical electron density (BCP properties and bond orders).

Table 6 Bonds strain factors δ calculated for zinc oxalate

ZnC_2O_4	δ_{Zn-O}	δ_{C-O}	δ_{C-C}	δ_{Struct}
	0.1389	0.3165	0.0006	0.2074
		δ_{C-O_1}	δ_{C-O_2}	
		0.2202	0.389607	

Conclusions

The main purpose of the undertaken studies, presented in this paper, was the attempt to analyze and explain, on a basis of the electronic structure, the way of thermal decomposition process in zinc anhydrous oxalate. In the analysis, we have used the results of *ab initio* calculations of band structure, density of states and electron density topology, in conjunction with calculated bond orders and bond valences. Despite the strong discrepancy between experimental and theoretical bond lengths, calculated from BVM model, which suggest the possibility of significant structure rebuilding after the process of breaking Zn–O_2^{ii} bonds (the longest bonds in structure), thus leading to potential uncertainty about most probable next steps in bond breaking process, the results of theoretically obtained electron density topology with related bond orders (especially $n_{CM(HL)}$) and bond valences, calculated from geometry of this compound, are consistent and allow us to predict with high reliability, the most probable sequence of bonds breaking during the process of thermal decomposition and thus its resulting products – zinc oxide, carbon oxide and carbon dioxide, in agreement with experiments [3, 28, 29]. The similar calculations have been carried out for cadmium and silver oxalates [19, 27] and their results have strongly supported and confirmed the experimental results of the way of thermal decomposition path for these two compounds (both decompose to metal and carbon dioxide).

Taking into account above conclusions, despite the general difficulty of predicting such complicated dynamical process like thermal decomposition using results of quantum stationary state calculations, we are convinced that such type of theoretical studies can be considered as a promising additional tool for analysis of the properties of the salts of carboxylic acids and their thermal decomposition reactions, enhancing our understanding of the processes taking place during such decomposition. Hence we plan to undertake subsequent studies for other isostructural compounds, searching for similarities and differences in their electronic structure and properties.

Acknowledgements

This work was supported by AGH-UST grant no 11.11.160.110

References

1 Y. D. Kondrashev, V. S. Bogdanov, S. N. Golubev and G. F. Pron, Zh. Struct. Khim., 26 (1985) 90.
2 E. Jeanneau, N. Audebrand and D. Louer, Acta Cryst., C57 (2001) 1012.
3 B. Małecka, E. Drożdż-Cieśla and A. Małecki, Thermochim. Acta, 423 (2004) 13.
4 M. E. Brown, D. Dollimore and A. K. Galwey, Comprehensive Chemical Kinetics, Vol. 22. Reactions In Solid State, C. H. Bamford and C. F. H. Tipper, Eds, Elsevier Amsterdam 1980.
5 V. V. Boldyrev, I. S. Nevyantsev, Y. I. Mikhailov and E. F. Khayretdinov, Kinet. Katal., 11 (1970) 367.
6 H. J. Borchardt and F. Daniels, J. Am. Chem. Soc., 79 (1957) 41.
7 D. Dollimore, Thermochim. Acta, 117 (1987) 331.
8 B. S. Randhawa and M. Kaur, J. Therm. Anal. Cal., 89 (2007) 251.
9 A. K. Galwey and M.E. Brown, J. Therm. Anal. Cal., 90 (2007) 9.

10 J. Fujita, K. Nakamoto and M. Kobayashi, J. Phys. Chem., 61 (1957) 1014.
11 S. Rane, H. Uskaikar, R. Pednekar and R. Mhalsikar, J. Therm. Anal. Cal., 90 (2007) 627.
12 P. Blaha, K. Schwarz, G. K. H. Madsen, D. Kvasnicka and J. Luitz, WIEN2k, An Augmented Plane Wave+Local Orbitals Program for Calculating Crystal Properties (Karlheinz Schwarz, Techn. Universität Wien, Austria), ISBN 3-9501031-1-2, (2001).
13 J. C. Slater, Phys. Rev., 51 (1937) 151.
14 T. L. Loucks, Augmented Plane Wave Method, Benjamin, New York 1967.
15 O. K. Andersen, Solid State Commun., 13 (1973) 133.
16 D. R. Hamann, Phys. Rev. Lett., 42 (1979) 662.
17 E. Wimmer, H. Krakauer, M. Weinert and A. J. Freeman, Phys. Rev., B24 (1981) 864.
18 D. J. Singh, Planewaves, Pseudopotentials and the LAPW Method, Kluwer Academic Publishers, Dordrecht 1994.
19 A. Koleżyński and A. Małecki, J. Therm. Anal. Cal., sent to editor.
20 J. P. Perdew, K. Burke and M. Ernzerhof, Phys. Rev. Lett., 77 (1996) 3865.
21 R. F.W. Bader, Atoms in Molecules: A Quantum Theory, Clarendon Press, Oxford 1990.
22 L. Pauling, The Nature of the Chemical Bond, Cornell University Press, Ithaca, New York 1960.
23 R. F. W. Bader, T. S. Slee, D. Cremer and E. Kraka, J. Am. Chem. Soc., 105 (1983) 5061.
24 J. Cioslowski and S. T. Mixon, J. Am. Chem. Soc., 113 (1991) 4142.
25 J. L. Jules and J. R. Lombardi, J. Mol. Struct. (Teochem.), 664–665 (2003) 255.
26 I. D. Brown, The Chemical Bond in Inorganic Chemistry. The Bond Valence Model., Oxford University Press, 2002.
27 A. Koleżyński and A. Małecki, J. Therm. Anal. Cal., sent to editor.
28 S. T. Howard and O. Lamarche, J. Phys. Org. Chem., 16 (2003) 133.
28 J. D. Danforth and J. Dix, J. Am. Chem. Soc., 93 (1971) 6843.
29 Z. Gabelica, R. Hubin and E. G. Derouane, Thermochim. Acta, 24 (1978) 315.

Received: September 5, 2008
Accepted: October 20, 2008
Online First: February 4, 2009

DOI: 10.1007/s10973-008-9494-0